AN ADVANCED SOLAR-ASSISTED CASCADE EJECTOR COOLING/CO_2 SUB-CRITICAL MECHANICAL COMPRESSION REFRIGERATION SYSTEM

V.O.Petrenko[1,2], B.J.Huang[1], K.O.Shestopalov[1,2], V.O.Ierin[2] and O.S.Volovyk[2]

[1] New Energy Center, Department of Mechanical Engineering, National Taiwan University, Taipei (Taiwan)

[2] Odessa State Academy of Refrigeration, Ejector Refrigeration Technology Center, Odessa (Ukraine)

volyablacksea@yandex.ru , volya@paco.net

1. Introduction

At the present time, the most prevalent cooling systems are electrically driven compression chillers, which have a world market share of about 90%. However, thermally powered cooling and refrigeration systems offer quite a number of interesting alternatives for use as air conditioners and refrigerators. This is especially true if they are driven by low-grade heat from solar collectors, thereby minimizing pollutant emissions and reducing primary energy consumption (Eicker, 2009).

Solar heat-driven ejector cooling machines (ECMs) realize refrigeration for air-conditioning, space-cooling, and food storage in the range of evaporating temperatures from 12ºC to –10ºC. These systems can be driven by conventional single-glazed flat plate solar collectors with selective surfaces and by vacuum tube solar collectors, which can be most economical for ECM with the proper choice of optimum generating temperature (Huang et al., 2001).

Low-grade heat-driven ECMs have advantages over other heat powered cooling and refrigeration cycles due to their simplicity in design, high reliability and durability, low installation cost and low maintenance and repair expenses. Recently, several high efficiency ECMs, operating with refrigerants R141b and R245fa, were developed that showed coefficients of performance (COPs) in the range of 0.5 – 0.7 under practical operating conditions. Achieved experimental results are very encouraging for air-conditioning and cooling applications because these COPs are similar to those of absorption cycle machines (Huang et al., 1999; Eames et al., 2007).

Hydrofluorocarbon refrigerants, which have been developed as alternatives to chlorofluorocarbon and hydrochlorofluorocarbon refrigerants, are known to have a high Global Warming Potential (GWP). For this reason environmentally benign, natural refrigerants are now attracting considerable attention. These natural refrigerants, which include ammonia, hydrocarbons, carbon dioxide, water, air, etc, have zero Ozone Depleting Potential and the majority of them have negligible GWP.

A distinctive feature of the system proposed in the present study is that it combines a conventional solar collector system and a cascade CO_2 sub-critical mechanical compression/heat-driven ejector cooling cycle that uses a hydrocarbon working fluid.

Carbon dioxide (CO_2) is a good refrigerant. The key advantages of CO_2 include the fact that it is easily available, environmental friendly, non-toxic, and not explosive. CO_2 has relatively high working pressures, which give a small vapor volume, which allows fabrication of compact components. The thermo-physical properties of carbon dioxide are excellent, its heat transfer coefficients are high and its sensitivity to pressure drop is low.

Since the critical temperature of CO_2 is rather low (31.1ºC), sub-critical operation is only possible when the average heat sink temperature is also rather low. In the event that sub-critical operation is feasible, CO_2 systems can compete very well in terms of energy efficiency with systems that use other refrigerants. In addition, CO_2 cycle performance and reliability can be significantly increased by reducing the discharge pressure. This also requires operation in the sub-critical mode (Robinson and Groll, 1998; Chen and Gu, 2005).

The present research aims to carry out a theoretical study for the design of a pilot small-scale cascade refrigeration cycle that utilizes a CO_2 sub-critical mechanical compression refrigerating machine (MCRM) and a solar powered ECM operating with a low-boiling environmentally friendly working fluid.

The analysis and comparison of performance characteristics for various low-boiling point refrigerants have shown that, from the thermodynamic and operating viewpoints, those most suitable for ECMs are low-pressure refrigerants that have high critical temperature T_{crit}, large specific latent heat at evaporating temperature T_e, small specific heat of liquid refrigerant in the range of operating temperatures ($T_g - T_e$) and normal boiling temperature $T_b \leq T_e$ (Petrenko, 2001; Petrenko et al., 2005a).

The calculations show that a number of hydrocarbons, such as R600, R600a, R601, R601a and R601b, have higher performances than other refrigerants. Consequently, the environmentally friendly refrigerant R601b (neopentane, C_5H_{12}), which has T_{crit} = 160.6ºC and T_e = 9.5 ºC, is selected as a promising working fluid for the solar-driven ECM in the present study.

2. Design of solar-assisted cascade refrigeration system

The present study develops an advanced solar-assisted cascade ejector cooling/CO_2 sub-critical mechanical compression refrigeration system. Fig. 1 shows the diagram of the proposed system, which consists of three main subsystems: a solar collector system, a low-grade heat-driven ECM, and a CO_2 sub-critical MCRM. The vacuum tube solar collector transforms solar radiation into thermal energy, which is then used to operate the ejector cooling cycle.

The ECM acts as the topping cycle and the MCRM acts as the bottoming cycle in the cascade system. The two cycles are thermally connected through the cascade condenser, which serves as the evaporator for the topping cycle and the condenser of the bottoming cycle.

The low-temperature (bottoming) cycle with CO_2 as working fluid can be used for refrigeration at temperature levels found suitable for supermarkets, cold storage rooms or food processing plants. The high-temperature (topping) cycle operating with neopentane as refrigerant is used to condense the CO_2 vapor of the low-temperature cycle in the cascade condenser.

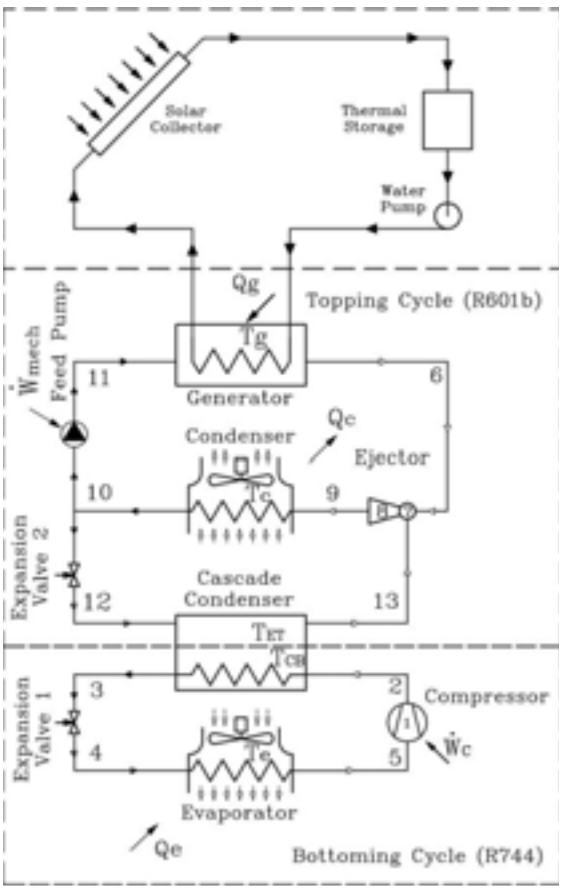

Fig.1: Diagram of a solar-assisted cascade ejector cooling/CO_2 sub-critical mechanical compression refrigeration system

In this way, the solar-driven ECM is used to cool the condenser of the MCRM to reduce its condensing temperature and thus to increase the performance of CO_2 cycle.

Fig. 2 shows the thermodynamic processes of the CO_2 and R601b cycles in *lgP-h* diagram. The operating principle of cascade refrigeration cycle is as follows. In the MCRM, the compressed carbon dioxide coming from the compressor is condensed in the cascade condenser at a condensing temperature T_{CB}. The liquid refrigerant then expands through an expansion valve 1 and enters the evaporator, where it is evaporated at low evaporating temperature T_e to produce the necessary cooling effect Q_e for refrigeration purposes. After the

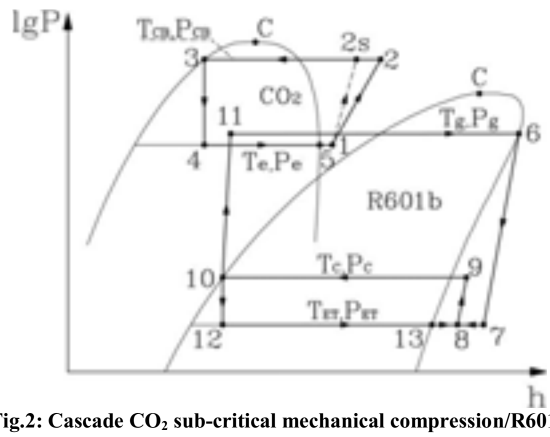

Fig.2: Cascade CO_2 sub-critical mechanical compression/R601b ejector cooling cycle in *lgP-h* diagram

evaporator, the entrained vapor is compressed to a high pressure state by the compressor, before entering the cascade condenser. This completes the CO_2 sub-critical mechanical compression refrigeration cycle.

Low grade heat Q_g is delivered from the solar collector to the generator of the ECM, where liquid refrigerant is vaporized at relatively high generating pressure P_g and temperature T_g. This primary vapor, with a mass flow rate of $\dot{m}_p$, flows through the primary convergent-divergent nozzle of the ejector and accelerates within it. At the exit of the nozzle, the accelerated flow becomes supersonic, and induces a locally low pressure region. The relatively low pressure produced by this expansion causes a suctioning effect of secondary flow, with a mass flow rate of $\dot{m}_s$, from the cascade condenser at low pressure P_{ET}. The primary and secondary fluids are mixed in the mixing section of the ejector and undergo a pressure recovery process in the diffuser section. The combined stream flows to the condenser where it is condensed to liquid at intermediate condensing pressure P_c and temperature T_c. The heat of condensation Q_c is rejected to the environment. The condensate is then divided into two parts – one is pumped back to the generator, and the other is expanded through an expansion valve 2 to a low-pressure state and enters the cascade condenser, where it is evaporated at low pressure P_{ET} and temperature T_{ET} by the condensation heat from the MCRM. The vapor is finally entrained by the ejector, thereby completing the exhaust heat driven ejector cooling cycle. The resulting cooling effect Q_{ET} is used to provide rejection of condensation heat from cascade condenser.

3. Analysis of ejector design and ejector cooling cycle performance

The supersonic ejector is the key component in the ejector cooling cycle. It is a simple jet device that is used in the ejector cycle for suction, compression and discharge of the secondary vapor by force of the primary vapor.

Fig. 3 illustrates the structure of a supersonic ejector with cylindrical (a) and conical-cylindrical (b) mixing chambers. The ejector assembly can be divided into four main parts: a nozzle, a suction chamber, a mixing chamber and a diffuser.

Operating conditions for the ejector are specified by operating pressures P_{ET}, P_c, P_g, expansion pressure ratio $E = P_g/P_e$ and compression pressure ratio $C = P_c/P_e$.

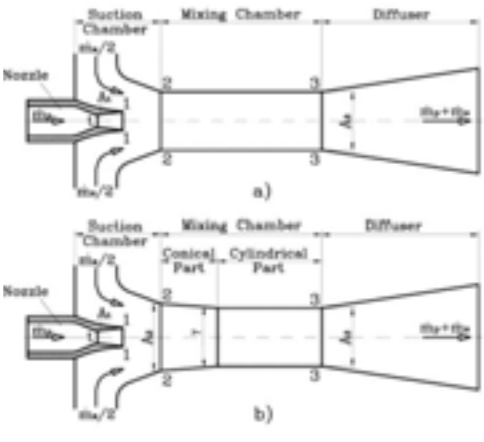

Fig.3: Structure of supersonic ejectors with cylindrical (a) and conical-cylindrical (b) mixing chambers

The performance of the ejector is measured by its entrainment ratio ω, which is the ratio between the secondary and the primary fluid mass flow rates $\dot{m}_s$ and $\dot{m}_p$, as shown in the following equation:

$$\omega = \frac{\dot{m}_s}{\dot{m}_p} \quad \text{(eq.1)}$$

The design of an ejector flow profile with a cylindrical mixing chamber is determined by the area ratio α, which is defined as the cross-section area of the cylindrical mixing section A_3 divided by that of the primary nozzle throat area A_t, which can be found from eq. (2):

$$\alpha = \frac{A_3}{A_t} \quad \text{(eq. 2)}$$

The design of a conical-cylindrical mixing chamber is specified by area ratio α, the converging angle γ at mixing chamber entrance and the area ratio β, which is defined as the entrance area A_2 of the conical part of mixing chamber divided by that of the cross-section area A_3, as shown in eq. (3):

$$\beta = \frac{A_2}{A_3} \quad \text{(eq. 3)}$$

Construction, geometry and surface condition of the supersonic ejector flow profile must provide the most effective utilization of primary flow energy for suction, compression and discharge of the secondary vapor (Huang et al., 2001; Petrenko, 1978; Petrenko, 2001; Petrenko et al., 2005b).

On the basis of the improved 1-D theory of ejector design, the area ratio α and the optimum value of β can be found with application of variational calculation. The value of β_{opt} corresponds to the maximum of entrainment ratio ω. Supplementary data for the determination of α, β_{opt} and the optimal converging angle γ are given in Petrenko (1978) and Petrenko et al. (2005a).

Theoretical and experimental investigations of supersonic ejectors with conical-cylindrical and cylindrical mixing chambers operating with various low-boiling refrigerants demonstrate convincingly that the application of conical-cylindrical mixing chambers at the same operating conditions causes an improvement of about 25-35% in ω compared with cylindrical mixing chambers. The advantage of ejectors with optimal design of conical-cylindrical mixing chambers is especially apparent at high critical condensing temperatures T_c (Petrenko, 1978; Petrenko et al., 2005b).

The performance of the ECM is usually measured by a single COP, which is the ratio of the useful cooling effect produced in the evaporator over the gross energy input into the ejector cycle required to produce the cooling effect. However, the fact that the ECM commonly utilizes a mechanical feed pump should be taken into account, as this consequently requires an input of some amount of mechanical power $\dot{W}_{mech}$ in addition to a low-grade thermal energy Q_g (Petrenko et al., 2005b; Petrenko, 2009). Although the mechanical power $\dot{W}_{mech}$, consumed by the feed pump is very small compared to the thermal energy Q_g input to the generator to actuate ejector, it may not be neglected (Petrenko, 2001).

Therefore, from both thermodynamic and economic points of view, the efficiency of the topping ECM cycle can be correctly characterized by separately using both thermal COP_{therm} and the actual specific power consumption of mechanical feed pump $\dot{w}_{mech}$. The value of COP_{therm} is defined as the cooling load at the cascade condenser Q_{ET} divided by the thermal energy Q_g, while the value of $\dot{w}_{mech}$ is the ratio between the mechanical power $\dot{W}_{mech}$ and the cooling effect Q_{ET}. These can be expressed as eqs. (4) and (5):

$$COP_{therm} = \frac{Q_{ET}}{Q_g} = \frac{\dot{m}_s q_{ET}}{\dot{m}_p q_g} = \omega \frac{q_{ET}}{q_g} \qquad \text{(eq. 4)}$$

$$\dot{w}_{mech} = \frac{\dot{W}_{mech}}{Q_{ET}} = \frac{\dot{m}_p v_5 \left(P_g - P_c\right)}{\eta_{pump}\, \dot{m}_s q_{ET}} = \frac{v_5 \left(P_g - P_c\right)}{\eta_{pump} \omega\, q_{ET}} \qquad \text{(eq. 5)}$$

where v_5 and η_{pump} are the specific volume of intake refrigerant and the feed pump coefficient of efficiency, respectively and $(P_g - P_c)$ is the generating and condensing pressure difference, kPa.

It should be observed that the electrically driven feed pump is the only component in the ejector cycle that has moving parts. Therefore, this component determines the reliability, leakproofness and lifetime of the whole system. Instead of using conventional electrically driven feed pumps for ECMs operating with flammable refrigerants such as neopentane, utilization of hermetic float-type thermo-gravity feeders, which are designed for application in various small capacity ejector systems, is very attractive (Petrenko et al., 2005b: Petrenko, 2009).

From the steady energy balance for the ECM using the numbering in Figs. 1 and 2, the cooling load at the cascade condenser Q_{ET}, the heat load at the generator Q_g, the heat load at the condenser Q_c and the actual power consumption of mechanical feed pump $\dot{W}_{mech}$ can be expressed as eqs. (6)-(9):

$$Q_{ET} = Q_{CB} = \left(h_{13} - h_{12}\right)\, \dot{m}_s \qquad \text{(eq. 6)}$$

$$Q_g = \left(h_6 - h_{11}\right)\, \dot{m}_p \qquad \text{(eq. 7)}$$

$$Q_c = Q_{ET} + Q_g = \left(h_9 - h_{10}\right)\left(\dot{m}_s + \dot{m}_p\right) \qquad \text{(eq. 8)}$$

$$\dot{W}_{mech} = \frac{\dot{m}_p v_5 \left(P_g - P_c\right)}{\eta_{pump}} \quad \text{(eq. 9)}$$

where h_{13} and h_{12}, h_6 and h_{11}, h_{10} and h_9 are the outlet and inlet refrigerant enthalpies at the cascade condenser, at the generator and at the condenser, respectively.

4. Simulation of solar ejector cooling cycle performance

In this study, we selected a vacuum tube solar collector which steady-state energy collection efficiency is calculated as follows: $\eta_{sc}=0.8\text{-}2.0(T_i\text{-}T_a)/I$, where I is the incident solar radiation on the tilted surface of the collector (W m^{-2}) and T_i and T_a are the collector inlet and the ambient temperatures (°C), respectively. The overall efficiency COP_o of the solar ECM is the product of the two particular coefficients:

$COP_o=COP_{therm}\times\eta_{sc}$ (eq. 10)

The selection of generating temperature T_g is especially important for solar ECM as it affects the COP_{therm} of the ECM as well as the solar collector efficiency η_{sc}. Since increases in T_g raise the COP_{therm} but lower the η_{sc}, the theoretical optimal T_g corresponds to a maximum COP_o that also will be determined in the present study (Huang et al., 2001).

The ejector and ECM performance was predicted by a computer simulation program based on the improved 1-D model of the ejector. This program calculates the performance of the ejector and ECM at critical-mode operating conditions and provides optimum design data for the ejector system (Huang et al., 1999; Petrenko at al., 2005a). The model validation against the experimental data for refrigerants R141b, R236fa and R245fa has shown very good agreement under a wide range of design and off-design operating conditions (Huang et al., 1999; Eames et al., 2004; Eames et al., 2007).

The program has been used for the theoretical study of the topping ejector cycle and supersonic ejector with conical-cylindrical mixing chambers, operating with R601b. For the present study, the ejector and the ECM were investigated over a wide range of T_g = 80–130°C, at T_c = 32, 36 and 40°C and at the fixed evaporating temperature T_{ET} = 16 ºC for application in the topping cycle of the cascade system.

The results of the analysis, shown in Figs. 4, 5, 6, 7, illustrate the variations of theoretical A_3/A_t, ω, COP_{therm} and $\dot{w}_{mech}$, with generating temperatures T_g at different critical condensing temperatures T_c for evaporating temperature T_{ET} =16°C. The area ratio A_3/A_t represents the design of the ejector. It is seen that the area ratio A_3/A_t increases with increasing T_g and decreasing T_c. The ω and COP_{therm} of the ECM also show the same trend. The characteristic $\dot{w}_{mech}$ decreases with both decreasing T_c and decreasing T_g (Petrenko, 2001).

Fig. 8 shows the variation in the solar collector efficiency η_{sc} with generating temperature T_g, and Fig. 9 shows the variation in overall COP_o with T_g for T_e = 16°C at T_c = 32, 36 and 40°C. Each curve in Fig. 9 has a broad peak, which corresponds to the theoretical optimum of generating temperature T_g. The optimum COP_o decreases with increasing T_c. For a higher performance efficiency of the solar collector η_{sc} the rated T_g can be chosen at temperatures about 10 to 15°C lower than the corresponding theoretical optimum values of T_g with only very little effect on COP_o (Huang et al., 2001).

For specified operating conditions T_e = 16°C and T_c = 36°C, the maximum COP_o = 0.284 and η_{sc} = 0.54 at a value of T_g = 115°C. However, the rated optimum of T_g has been chosen 15°C lower – that is, 100°C – with η_{sc} = 0.57 and COP_o = 0.282, which is 0.7% smaller than the maximum COP_o.

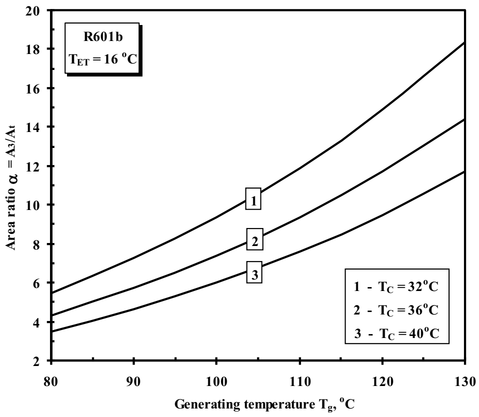

Fig. 4: Variations in A_3/A_t with T_g at different T_c

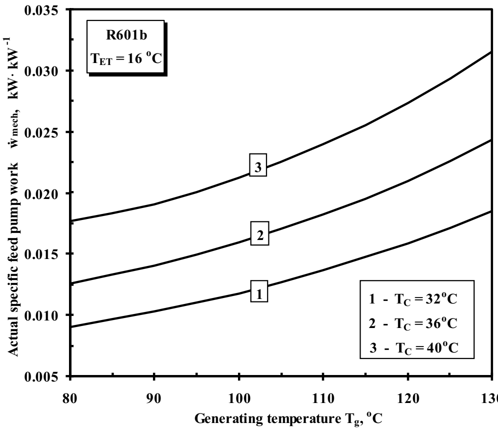

Fig. 7: Variations in $\dot{W}_{mech}$ with T_g at different T_c

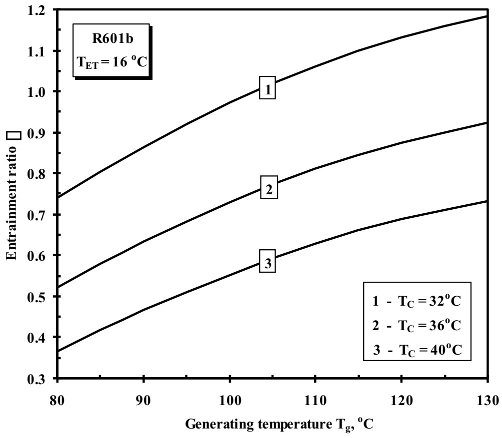

Fig. 5: Variations in ϖ with T_g at different T_c

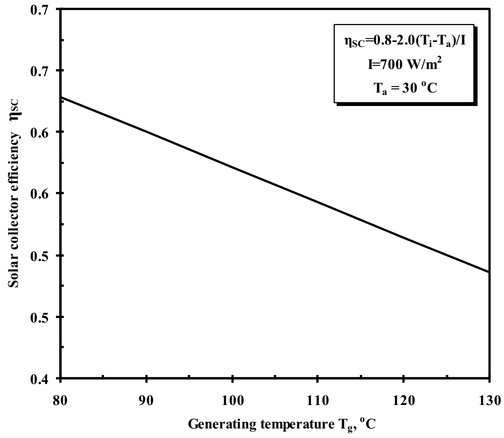

Fig. 8: Variation in solar collector efficiency η_{sc} with T_g

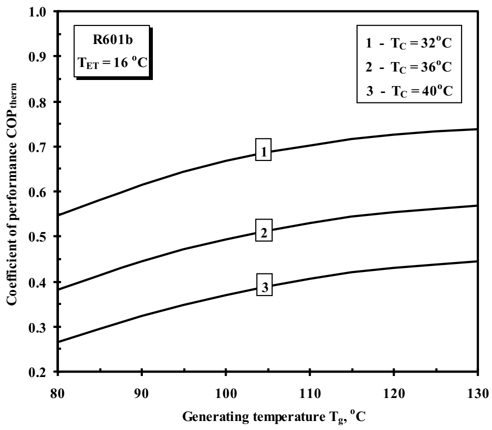

Fig. 6: Variations in COP_{therm} with T_g at different T_c

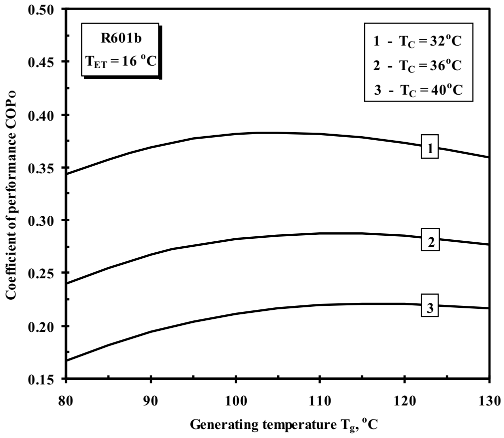

Fig. 9: Variations in overall COP_o with T_g at different T_c

5. Analysis of CO_2 sub-critical compression refrigeration cycle

Analysis of the CO_2 sub-critical mechanical compression refrigeration cycle is described as follows. From the steady energy balance for the MCRM and using the numbers in Figs. 1 and 2, a specific cooling capacity q_e, a specific condensing heat q_{CB} and a specific isentropic compressor work l_{cs} may be computed by eqs. (11)-(13):

$$q_e = h_5 - h_4 \quad \text{(eq. 11)}$$

$$q_{CB} = h_2 - h_3 \quad \text{(eq. 12)}$$

$$l_{cs} = h_{2s} - h_1 \quad \text{(eq. 13)}$$

where h_5 and h_4, h_3 and h_2, h_{2s} and h_1 are the outlet and inlet refrigerant enthalpies at the evaporator, at the cascade condenser and at the compressor, respectively.

Actual work of the compressor is defined as follows:

$$l_C = h_2 - h_1 = (h_{2s} - h_1)/\eta_{cs} \quad \text{(eq. 14)}$$

where η_{cs} is the isentropic efficiency of the compressor.

The enthalpy of the outlet of the compressor can be expressed as eq. (15):

$$h_2 = h_1 + \frac{h_{2s} - h_1}{\eta_{cs}} \quad \text{(eq. 15)}$$

For the chosen semi-hermetic CO_2 type compressor, η_{cs} can be written as a function of the ratio of compressor discharge and suction pressures $r = P_{CB}/P_e$. The correlation obtained by best fitting the experimental data for the CO_2 sub-critical refrigeration cycle (Neksa et al., 2001) has the following form:

$$\eta_{cs} = 0.8981 - 0.09238\, r + 0{,}00476\, r^2 \quad \text{(eq. 16)}$$

The CO_2 cycle coefficient of performance is defined as the specific cooling effect at the evaporator q_e, divided by the actual specific compressor work l_C, as shown in eq. (17):

$$COP_{BC} = \frac{q_e}{l_C} = \frac{h_5 - h_4}{h_2 - h_1} \quad \text{(eq. 17)}$$

The values of the refrigeration output of the compression cycle Q_e, the compressor power consumption $\dot{W}_C$ and the heat load at the cascade condenser Q_{CB} are found respectively from eqs. (18)-(20):

$$Q_e = q_e\, \dot{m} \quad \text{(eq. 18)}$$

$$\dot{W}_C = l_C\, \dot{m} \quad \text{(eq. 19)}$$

$$Q_{CB} = q_{CB}\, \dot{m} = Q_e + \dot{W}_C = Q_{ET} \quad \text{(eq. 20)}$$

where $\dot{m}$ is the mass flow rate of CO_2 in the bottoming cycle.

Internal superheating caused by the semi-hermetic compressor motor can be calculated from eq. (21):

$$\Delta T_{sup} = T_1 - T_5 = \frac{1}{c_p}(h_2 - h_1)\left(\frac{1}{\eta_m} - 1\right) \quad \text{(eq. 21)}$$

where c_p is constant pressure specific heat of CO_2 and η_m is the coefficient of efficiency of the motor.

All calculations were performed using the REFPROP 8.0 (Lemmon et al., 2007).

6. Results and discussion

The CO_2 sub-critical cycle at the presented stage of the design-theoretical study has been investigated with fixed cooling capacity Q_e = 5 kW and a fixed condensing temperature T_{CB} = 21°C, with a specified temperature difference $\Delta T = T_{CB} - T_{ET}$ = 5°C in the CO_2/R601b cascade condenser. The evaporating temperatures T_e used in the parametric study are taken in the range from -30 to 10°C, with assumed internal superheating ΔT_{sup} of 10°C in the semi-hermetic compressor.

Fig. 10 shows the variations of Q_{CB} and $\dot{W}_C$ with T_e of MCRM for Q_e = 5 kW at T_{CB} = 21°C. As seen in Fig. 10, both Q_{CB} and $\dot{W}_C$ decrease with increasing T_e.

Fig. 11 illustrates the variations of COP_{BC} with T_e for $Q_e = 5$ kW at $T_{CB} = 21$°C. The increase in T_e results in a rise in the COP_{BC} of the bottoming cycle. The COP_{BC} clearly increases, from 1.56 to 12.27, when the T_e varies from -30°C to 10°C.

Fig. 12 shows variation in the solar collector area A_{sc} with T_e, which can be found from eq. (22):

$$A_{sc} = \frac{Q_{ET}}{COP_{therm}\,\eta_{sc}\,I} = \frac{Q_{BC}}{COP_o\,I} = \frac{Q_e + \dot{W}_C}{COP_o\,I} \quad \text{(eq. 22)}$$

Fig. 12 indicates that for $Q_e = 5$ kW at $T_{CB} = 21$°C, a decrease in T_e and an increase in T_c results in a rise in the solar collector area A_{sc}.

Figs. 13 – 15 show the influence of the evaporating temperature T_e on the heat loads Q_{ET}, Q_g, Q_c, mass flow rates $\dot{m}_s$ and $\dot{m}_p$ of the ECM cycle and areas A_t and A_3 of the ejector with β_{opt} for $Q_e = 5$ kW at $T_{CB} = 21$°C, $T_{ET} = 16$°C, $T_c = 36$°C, $T_g = 100$°C.

From Figs. 12 – 15 it is seen that T_e affects the bottoming MCRM CO_2 cycle as well as the topping ECM cycle operating with neopentane and the solar collector area A_{sc}.

Referring to Figs. 13 and 14, the heat loads Q_{ET}, Q_g, Q_c and mass flow rates $\dot{m}_s$ and $\dot{m}_p$ show the same trend: notably, they decrease with the increasing in T_e.

Fig. 14 shows that A_t reduces very slowly and almost linearly with increasing T_e, while A_3 falls more rapidly.

On the basis of the obtained results, a pilot small-scale cascade CO_2 sub-critical mechanical compression/neopentane ejector refrigerating unit was developed with a cooling capacity of 5 kW. A diagram of this unit is shown in Fig. 16, and the design performance characteristics of its CO_2 bottoming cycle and R601b topping cycle are listed in Table 1.

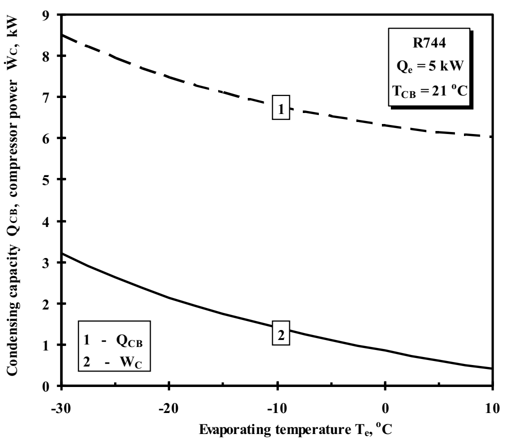

Fig.10: Variation in Q_{CB} and $\dot{W}_C$ with T_e for $Q_e = 5$ kW at $T_{CB} = 21$°C

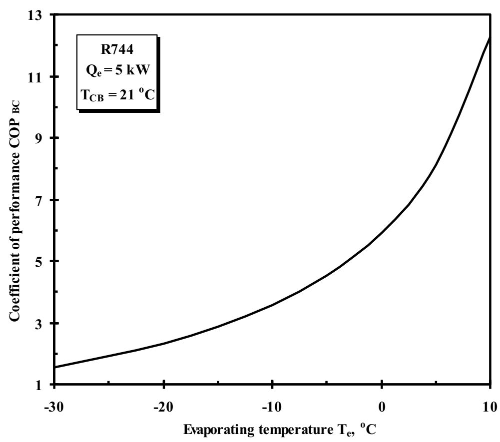

Fig.11: Variation in COP_{BC} with T_e for $Q_e = 5$ kW at $T_{CB} = 21$°C

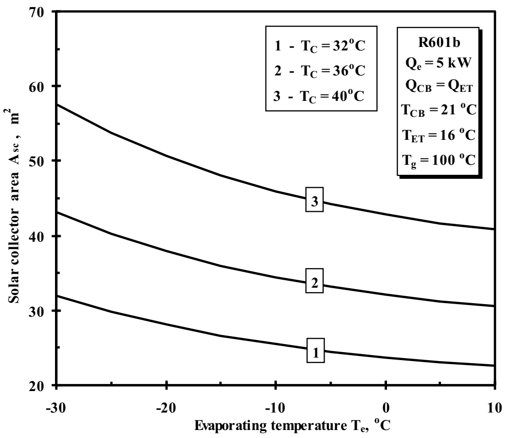

Fig. 12: Variations in A_{sc} with T_e at different T_c

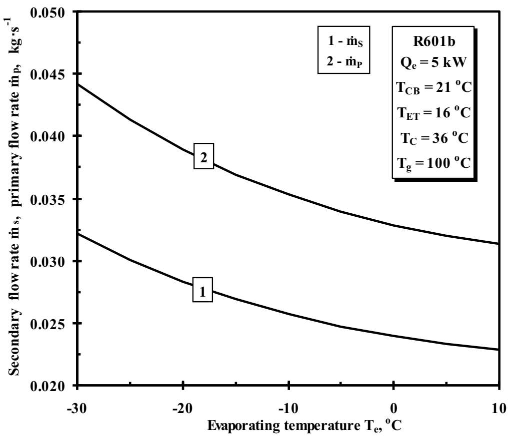

Fig.14: Variation in $\dot{m}_S$ and $\dot{m}_P$ with T_e for $Q_e = 5$ kW at $T_{CB} = 21°C$, $T_{ET} = 16°C$, $T_c = 36°C$, $T_g = 100°C$

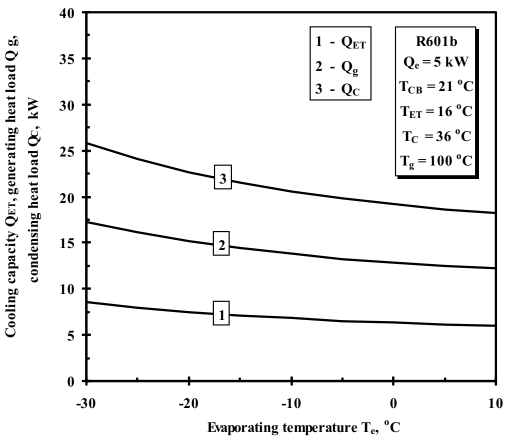

Fig.13: Variation in Q_{ET}, Q_c and Q_g with T_e for $Q_e = 5$ kW at $T_{CB} = 21°C$, $T_{ET} = 16°C$, $T_c = 36°C$, $T_g = 100°C$

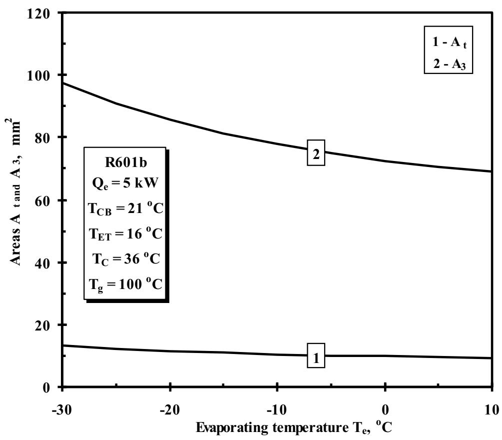

Fig.15: Variation in A_t and A_3 with T_e for $Q_e = 5$ kW at $T_{CB} = 21°C$, $T_{ET} = 16°C$, $T_c = 36°C$, $T_g = 100°C$

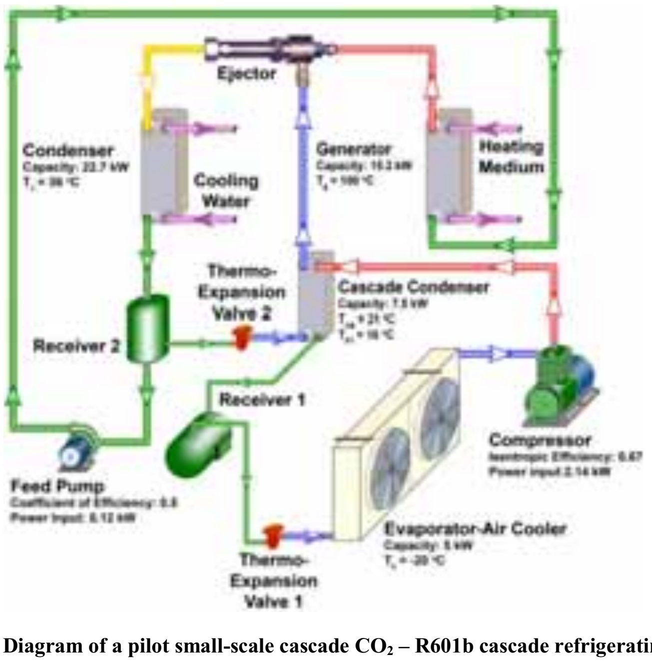

Fig.16: Diagram of a pilot small-scale cascade CO_2 – R601b cascade refrigerating unit

Tab. 1: **Design performance specifications of the CO_2 – R601b cascade refrigerating unit**

Parameter	Value
Bottoming cycle (R744)	
Cooling capacity, Q_e	5 kW
Evaporating temperature, T_e	-20 °C
Evaporating pressure, P_e	19.7 bar
Compressor power input, $\dot{W}_C$	2.14 kW
Superheating capacity in motor, Q_{sup}	0.36 kW
Condensing heat load, Q_{CB}	7.5 kW
Condensing temperature, T_{CB}	21 °C
Condensing pressure, P_{CB}	58.7 bar
Compressor type	semi-hermetic
Compressor isentropic efficiency, η_{is}	0.67
Design $COP_{BC} = Q_e/\dot{W}_C$	2.33
Topping cycle (R601b)	
Cooling capacity, $Q_{ET} = Q_{CB}$	7.5 kW
Evaporating temperature, T_{ET}	16 °C
Evaporating pressure, P_{ET}	1.27 bar
Condensing heat load, Q_c	22.7 kW
Condensing temperature, T_c	36 °C
Condensing pressure, P_c	2.4 bar
Generating heat load, Q_g	15.2 kW
Generating temperature, T_g	100 °C
Generating pressure, P_g	11.19 bar
Entrainment ratio, $\omega = \dot{m}_s/\dot{m}_p$	0.73
Design $COP_{therm} = Q_{ET}/Q_g$	0.49
Pressure difference, P_g-P_c	8.79 bar
Feed pump power input, $\dot{W}_{mech}$	0.12 kW
Actual specific work of feed pump, $\dot{w}_{mech}$	0.016 kW kW^{-1}
Feed pump coefficient of efficiency, η_{pump}	0.5
Design area ratio $\alpha = A_3/A_t$	7.4
Design optimal area ratio $\beta_{opt} = A_2/A_3$	1.16
Solar collector efficiency, η_{sc}	0.57
Rated $COP_o = COP_{therm} \times \eta_{sc}$	0.28
Solar collector area, A_{sc}	38.1 m^2

Obtained technical data may serve as guidelines in the design of full-scale cascade CO_2 sub-critical mechanical compression/neopentane ejector refrigerating units with other cooling capacities.

7. Conclusion

In this paper an innovative solar-assisted cascade refrigeration system, composed of a solar collector system and a cascade refrigeration cycle, is proposed. The solar collector system is a system for heat production. The cascade refrigeration cycle is the combination of a MCRM, operating with CO_2, and an ECM, driven by solar energy and using neopentane as the working fluid.

According to theoretical study for the design of a small-scale solar-assisted cascade CO_2 – R601b refrigerating unit the most important findings are as follows:

- The effect of the cascade cycle operating conditions on solar ECM and MCRM cycle performance characteristics is studied and optimal geometry of the ejector is determined.

- The obtained data provide necessary information to design a pilot small-scale CO_2 – R601b solar-assisted cascade refrigerating unit with cooling capacity of 5 kW.

- The proposed solar-assisted cascade refrigeration system is environmentally friendly, energy saving and a potentially high performance and cost-beneficial installation that consolidates the advantages of both ECM and MCRM cycles.

Acknowledgements

This publication is based on the work supported by Award No.KUK-C1-014-12, made by King Abdullah University of Science and Technology (KAUST), Saudi Arabia.

References

Chen, Y., Gu, J., 2005. The optimum high pressure for CO_2 transcritical refrigeration systems with internal heat exchangers. International Journal of Refrigeration 28, 1238–1249.

Eames, I.W., Ablwaifa, A.E., Petrenko, V.O., 2007. Results of an experimental study of an advanced jet-pump refrigerator operating with R245fa. Applied Thermal Engineering 27, 2833-2840.

Eames, I.W., Petrenko, V.O., Ablwaifa, A.E., 2004. Design and experimental investigation of a jet pump refrigerator. 3rd International Conference on Heat Powered Cycles – HPC Larnaca, Cyprus.

Eicker U. 2009, Low Energy Cooling for Sustainable Buildings, John Wiley & Sons, Chichester, 264 p.

Huang, B.J., Chang, J.M., Wang, C.P., Petrenko, V.O., 1999. A 1-D analysis of ejector performance. International Journal of Refrigeration 22, 368-378.

Huang, B.J., Petrenko, V.O., Samofatov, I.Y., Shchetinina, N.A., 2001. Collector selection for solar ejector cooling systems. Solar Energy 71, 269-274.

Lemmon, E.W., Huber, M.L., McLinden, M.O., 2007. NIST Standard Reference Database 23: Reference Fluid Thermodynamic and Transport Properties-REFPROP, Version 8.0. National Institute of Standards and Technology, Standard Reference Data Program, Gaithersburg.

Neksa, P., Dorin, F., Rekstad, H., Bredesen, A., 2001. Measurements and experience on semi-hermetic CO_2 compressors. 4th International Conference on Compressors and Coolants. IIR, Slovak Republic.

Petrenko, V.O., 1978. Investigation of ejector cooling machine operating with refrigerant R142b. Ph.D. thesis. Odessa Technological Institute of Refrigeration Industry, Ukraine.

Petrenko, V.O., 2001. Principle of working fluid selection for ejector refrigeration systems. Refrigeration Engineering and Technology 1 (70), 16-21.

Petrenko, V.O., 2009. Application of innovative ejector chillers and air conditioners operating with low-boiling refrigerants in trigeneration systems. EUROTHERM SEMINAR №85, Louvain-la-Neuve, Belgium.

Petrenko, V.O., Chumak, I.G., Volovyk, O.S., 2005a. Comparative analysis of the performance characteristics of an ejector refrigerating machine utilizing various low-boiling working fluids. Refrigeration Engineering and Technology 5 (97), 25-35.

Petrenko, V.O., Volovyk, O.S., Ierin, V.O., 2005b. Areas of effective application of ejector refrigeration machines using low-boiling refrigerants. Refrigeration Engineering and Technology 1, 17-30.

Robinson, D.M., Groll, E.A., 1998. Efficiencies of transcritical CO_2 cycles with and without an expansion turbine. International Journal of Refrigeration 21(7), 577-589.